Science Translational Medicine
AAAS

www.sciencetranslationalmedicine.org/cgi/content/full/9/377/eaag1809/DC1

Supplementary Materials for

Delayed differentiation of potent effector CD8$^+$ T cells reducing viremia and reservoir seeding in acute HIV infection

Hiroshi Takata, Supranee Buranapraditkun, Cari Kessing, James L. K. Fletcher, Roshell Muir, Virginie Tardif, Pearline Cartwright, Claire Vandergeeten, Wendy Bakeman, Carmen N. Nichols, Suteeraporn Pinyakorn, Pokrath Hansasuta, Eugene Kroon, Thep Chalermchai, Robert O'Connell, Jerome Kim, Nittaya Phanuphak, Merlin L. Robb, Nelson L. Michael, Nicolas Chomont, Elias K. Haddad, Jintanat Ananworanich, Lydie Trautmann,* on behalf of the RV254/SEARCH010 and the RV304/SEARCH013 Study Groups

*Corresponding author. Email: ltrautmann@hivresearch.org

Published 15 February 2017, *Sci. Transl. Med.* **9**, eaag1809 (2017)
DOI: 10.1126/scitranslmed.aag1809

The PDF file includes:

Other Supplementary Material for this manuscript includes the following:
(available at www.sciencetranslationalmedicine.org/cgi/content/full/9/377/eaag1809/DC1)

Table S1 (Microsoft Excel format). Primary data.

Materials and Methods

Antibodies and reagents for flow cytometry

FITC-labeled Annexin V, FITC-labeled anti-Bcl-2, PE-Cy7-labeled anti-CCR7, PE-CF594-labeled anti-CCR7, PE-labeled anti-CCR7, BUV737-labeled anti-CD127, PE-CF594-labeled anti-CD127, allophycocyanin H7-labeled anti-CD27, BV711-labeled anti-CD27, Alexa Fluor 700-labeled anti-CD3, allophycocyanin H7-labeled anti-CD45RA, BUV395-labeled anti-CD8, PE-Cy7-labeled anti-HLA-DR, PerCP-Cy5.5-labeled anti-IL-2, BV786-labeled anti-Ki-67, PE-CF594-labeled anti-T-bet mAbs, GolgiPlug and Perm/Wash Buffer were obtained from BD Biosciences. Pacific Blue-labeled Annexin V, BV650-labeled anti-CD127, BV650-labeled anti-CD27, allophycocyanin-labeled anti-CD38, BV650-labeled anti-CD38, BV605-labeled anti-CD4, BV650-labeled anti-CD45RA, BV785-labeled anti-CD8, Pacific Blue-labeled anti-CD8, PerCP-Cy5.5-labeled anti-HLA-DR, BV711-labeled anti-HLA-DR, Pacific Blue-labeled anti-IFN-γ, BV421-labeled anti-Ki-67, BV711-labeled anti-Ki-67, Pacific Blue-labeled anti-Perforin, and PE-labeled anti-TNF-α mAbs came from BioLegend. PerCP-eFluor710- labeled anti-EOMES and Foxp3/ Transcription Factor Staining Buffer Set were from eBioscience. HLA-A*1101 EBV EBNA 3B (AVFDRKSDAK and IVTDFSVIK) dextramers were purchased from IMMUDEX. HLA-A*1101 HIV-1 NEF (GAFDLSFFLK and QVPLRPMTYK), and HLA-A*1101 HIV-1 POL (AIFQSSMTKIL) soluble biotinylated monomers were produced at Chulalongkorn University (Bangkok, Thailand) as previously described (57) and tetramerized with PE-conjugated extravidin (Sigma-Aldrich). LIVE/DEAD Fixable Aqua Dead Cell Stain Kit (LIVE/DEAD), MitoTracker Green FM, MitoTracker Orange CM-H_2TMRos, CellROX Deep Red, and CountBright Absolute Counting Beads were from Thermo Fisher Scientific (Molecular Probes).

Flow cytometry analysis

For general phenotyping, thawed PBMCs were first stained with cell surface markers at 4°C for 20 minutes. They were washed with PBS containing 2% FBS (washing buffer) twice, and then fixed and permeabilized with Foxp3/ Transcription Factor Staining Buffer Set. The cells were stained with anti-Bcl-2, anti-Ki-67, anti-Perforin, and anti-T-bet mAbs at room temperature for 30 minutes followed by 2 times wash with Foxp3 permeabilization buffer and washing buffer, respectively. For phenotypic analysis on antigen specific $CD8^+$ T cells, thawed PBMCs were first stained with PE-labeled pMHC tetramer/ dextramer at 37°C for 15 minutes. The cells were stained for the other cell surface markers at 4°C for 20 minutes followed by 2 times wash with washing buffer. The cells were fixed/ permeabilized and stained for Bcl-2, Ki-67, Perforin, and T-bet as mentioned earlier. To analyze cytokine productivity in $CD38^+HLA\text{-}DR^+$ $CD8^+$ T cells, thawed PBMCs were plated at $2x10^6$ cells/ well in 24 well tissue culture plates which were pre-coated with anti-CD3 mAb (clone: OKT3) at 5μg/ml. The cells were stimulated in media containing GolgiPlug (Brefeldin A) and soluble anti-CD28 mAb (clone: CD28.2) at 0.5μg/ml for 8 hrs. The cells were harvested after the stimulation, and stained

for cell surface markers. After 2 times wash with washing buffer, the cells were fixed in PBS containing 2% formaldehyde, and then permeabilized with Perm/Wash Buffer according to the manufacture's protocol. The cells were stained with anti-IFN-γ, anti-TNF-α, and anti-IL-2 mAbs at room temperature for 30 minutes followed by 2 times wash with Perm/Wash Buffer and wash buffer, respectively. To analyze cell survival capacity, $CD8^+$ T cells were negatively isolated from thawed PBMCs by using human $CD8^+$ T cell enrichment kit (StemCell Technologies). The purified $CD8^+$ T cells were stained immediately (*ex vivo*) or after 24 hours of culture for cell surface markers. After 2 times wash with washing buffer, the cells were stained with LIVE/DEAD and Annexin V in Annexin V binding buffer (BD Biosciences) at room temperature for 15 minutes. After 2 times wash with Annexin V binding buffer, CountBright beads were added to all the samples before flow cytometry analysis, and the survived cell number was normalized based on recorded number of the CountBright beads on a cytometer. To analyze mitochondrial profile, thawed PBMCs were first rested at 37°C for 10 minutes, and then they were stained with MitoTracker Green, MitoTracker Orange CM-H_2TMRos, and CellROX Deep Red according to the manufacture's protocol. After 2 times wash with RPMI-1640 supplement with 10% FBS, the cells were stained with cell surface markers and Annexin V as described earlier. The cells were analyzed without fixation on FACS AriaII (BD Biosciences). All the stained cells were resuspended in PBS containing 2% formaldehyde before analysis on LSRII (BD Biosciences) except for mitochondrial staining. All the flow cytometry data were analyzed with FlowJo v10 (FlowJo, LLC).

Gene expression analysis

Gene specific Primers and Probes were designed using the Roche Universal Probe Library Assay Design Center (www.universalprobelibrary.com) and were designed to detect multiple transcripts, without respect to isoform prevalence. PBMCs were stained for cell surface markers, and $CD38^+HLA\text{-}DR^+$ cells in $CD45RA^-$ $CD8^+$ T cells were directly sorted into 96 PCR plates by FACS AriaII. The cells were reverse transcribed and amplified in a single-step RT-Specific Template Amplification (STA) using a pool of all the primer sets and with the Superscript III Platinum One-Step qRT-PCR Kit (Thermo Fisher Scientific, Life Technologies). The STA was carried out for 18 cycles of 95°C for 15 seconds and 60°C for 4 minutes. Unincorporated primers and any generated non-specific single-stranded products were then removed by an Exonuclease I (New England Biolabs). High-throughput qPCR on the pre-amplified samples was performed on a 96.96 BioMark™ Dynamic Array (Fluidigm) for 40 cycles as previously described (58). The same primer set used in the RT-STA was used for the probe-based qPCR. Threshold cycle (Ct) values were calculated by the Real-Time PCR Analysis Software (Fluidigm) and failed reactions were discarded from the analysis. Target gene Ct value was normalized based on the geometric mean of Ct values for 2 house keeping genes (RPL13A and IPO8) as previously described (*56*). The lowest expression Ct value in each gene was used as a calibrator to calculate relative mRNA expression levels.

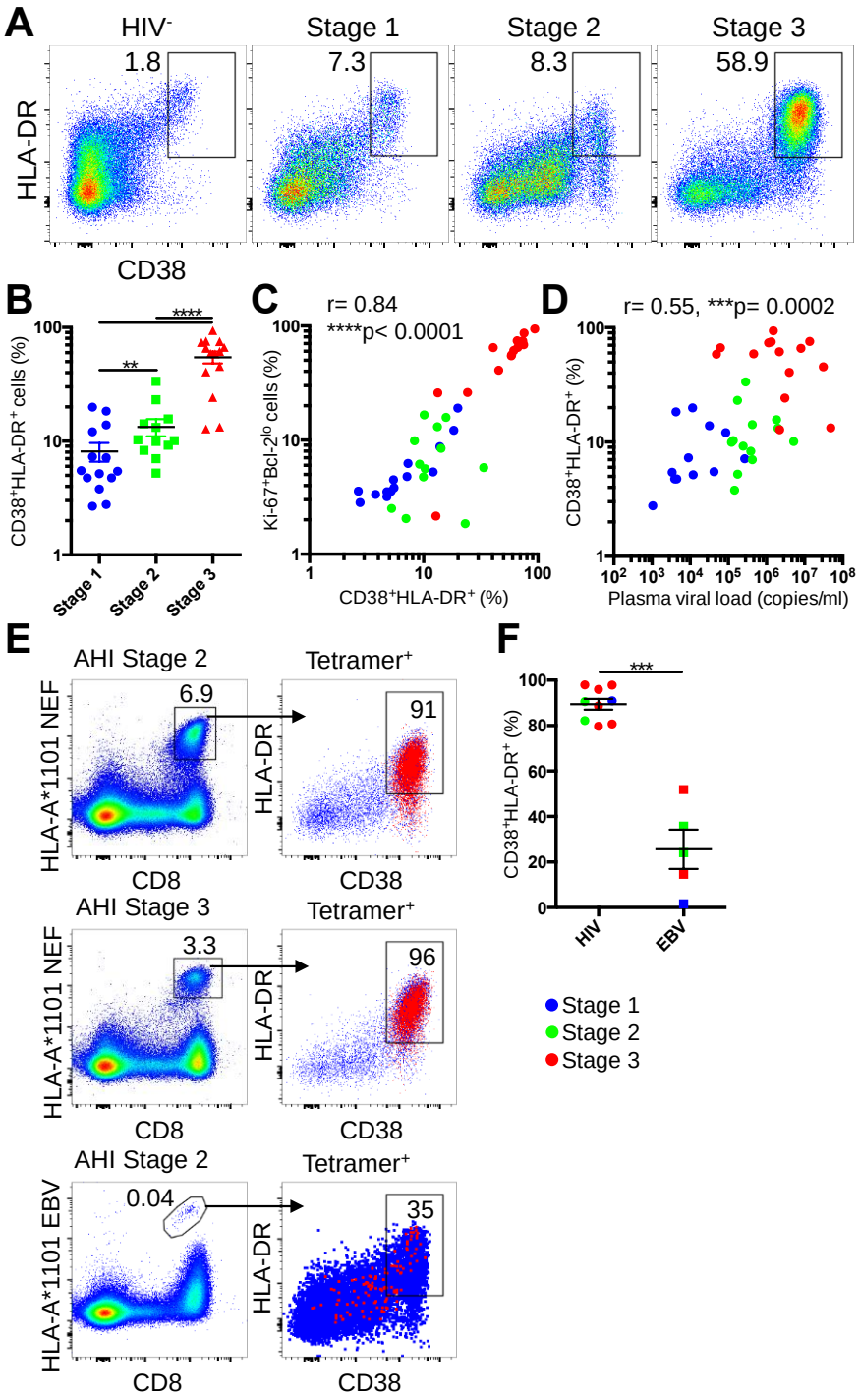

Fig. S1. HIV-specific CD8⁺ T cell expansion in AHI. (A) Representative dot plot of CD38⁺HLA-DR⁺ CD8⁺ T cells. (B) Percentages of CD38⁺HLA-DR⁺ cells in CD45RA⁻CD8⁺ T cells from HIV- and AHI 4thG Stages 1-3 individuals. (C) Correlation between percentage of Ki-67⁺Bcl-2lo and CD38⁺HLA-DR⁺ CD8⁺ T cells. (D) Correlation between plasma viral load and percentages of CD38⁺HLA-DR⁺ CD8⁺ T cells. (E) Representative dot plot of HLA-A*1101 NEF or EBV tetramer⁺ CD8⁺ T cells gated on total live PBLs (Left). Overlay of CD38⁺HLA-DR⁺ expression on tetramer⁺ (Red) and total CD45RA⁻CD8⁺ T cells (Blue) from the same individuals (Right). (F) Percentage of CD38⁺HLA-DR⁺ in HIV or EBV tetramer⁺ cells from AHI stage 1-3 individuals. Differences between groups were analyzed by Mann-Whitney tests. Associations between two variables (p and r) were analyzed by Spearman correlations. **P< 0.01; ***P< 0.001; ****P< 0.0001.

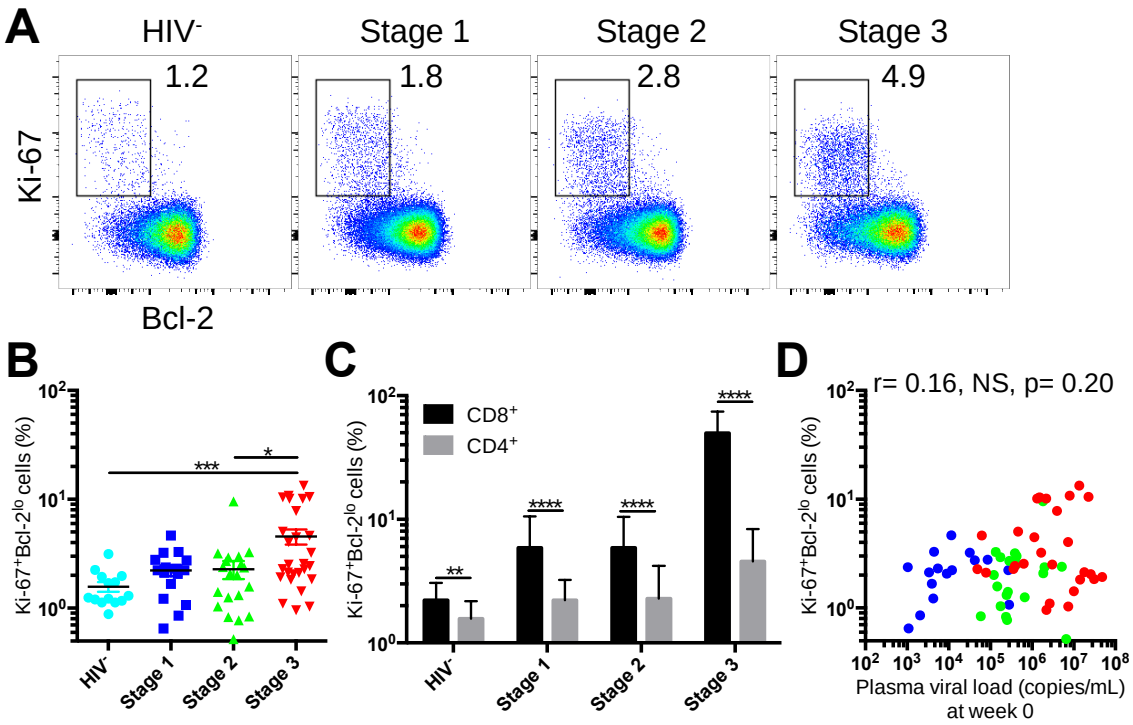

Fig. S2. CD4$^+$ T cell activation in acute HIV-1 infection. (A) Representative dot plot of Ki-67$^+$Bcl-2^{lo} CD4$^+$ T cells. (B) Percentages of Ki-67$^+$Bcl-2^{lo} cells in CD45RA$^-$CD4$^+$ T cells from 14 HIV- and 16 AHI 4thG Stages 1, 20 Stage 2, and 27 stage 3 individuals. (C) Comparison between percentages of Ki-67$^+$Bcl-2^{lo} cells in CD45RA$^-$ CD4$^+$ T cells and that in CD45RA$^-$CD8$^+$ T cells. (D) Correlation between plasma viral load and percentages of Ki-67$^+$Bcl-2^{lo} CD4$^+$ T cells. Differences between groups were analyzed by Mann-Whitney tests. Associations between two variables (p and r) were analyzed by Spearman correlations. *P< 0.05; **P< 0.01; ***P< 0.001; ****P< 0.0001.

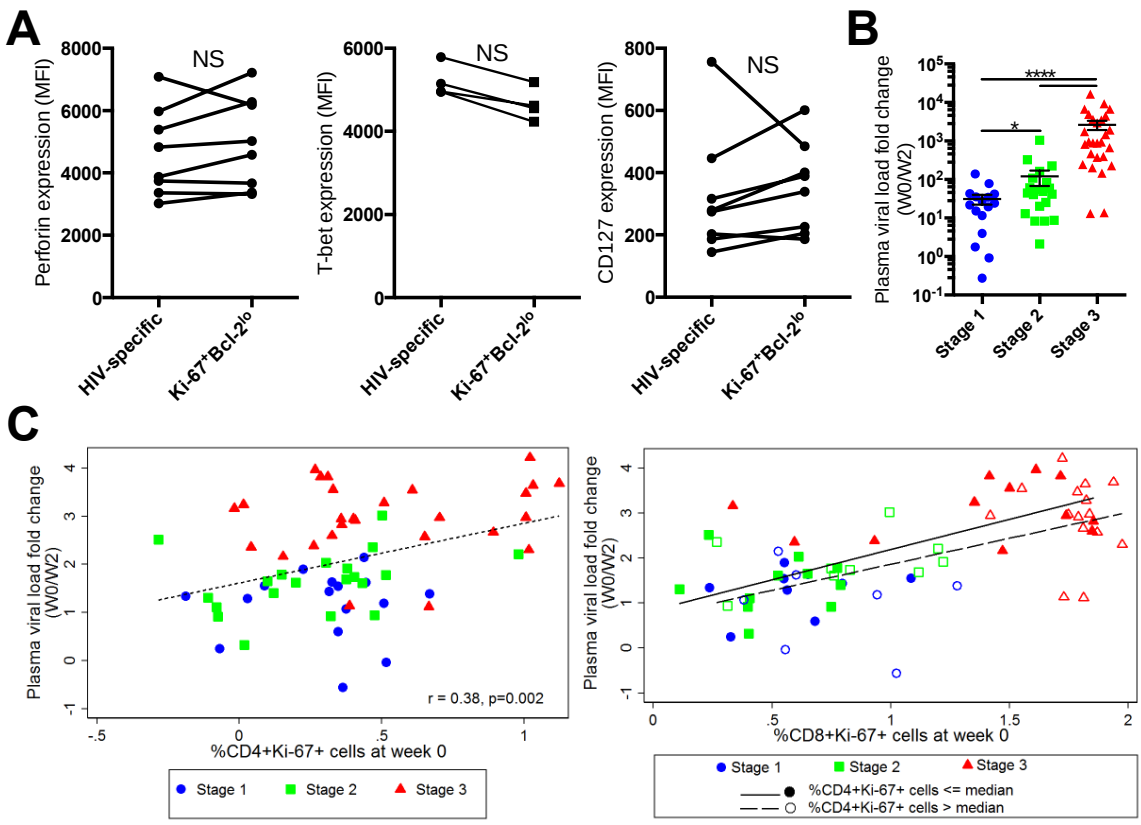

b coefficients and 95%CI obtained from the linear regression model

Parameters	Univariate		Multivariate	
	b Coefficient (95%CI)	p-value	b Coefficient (95%CI)	p-value
CD8+Ki-67+ cells	0.02 (0.01 – 0.03)	<0.001	0.02 (0.01 to 0.03)	<0.001
CD4+Ki-67+ cells	0.15 (0.06 – 0.23)	0.001	0.02 (-0.08 to 0.12)	0.67
			Adjusted correlation coefficient (r)	0.56 (p=0.001)

Fig. S3. Characteristics of effector CD8$^+$ T cells and plasma viral load during different stages of AHI. (A) Expression of perforin, T-bet, and CD127 on HIV-specific tetramer$^+$ cells and Ki-67$^+$Bcl-2^{lo} CD45RA$^-$CD8$^+$ T cells from the same individuals in AHI. Differences between HIV-specific and Ki-67$^+$Bcl-2^{lo} cells were analyzed by Wilcoxon test. (B) Plasma viral load fold change in individuals between week 0 and week 2 after initiating ART at different AHI stages. Differences between groups were analyzed by Mann-Whitney tests. *P< 0.05; ****P< 0.0001. (C) Correlation between plasma viral load fold change (week 0/ week 2) and percentage of Ki-67$^+$Bcl-2^{lo} cells in CD45RA$^-$CD4$^+$ T cells or that in CD45RA$^-$CD8$^+$ T cells at week 0. By utilizing Multivariate linear regression model, percentage of Ki-67$^+$CD4$^+$ T cells were added to the existing model of plasma viral load fold change and Percentage of Ki-67$^+$CD8$^+$ T cells. The regression lines from the individuals have high (>median) and low (≤median) percentage of CD4$^+$Ki-67$^+$ cells are compared.

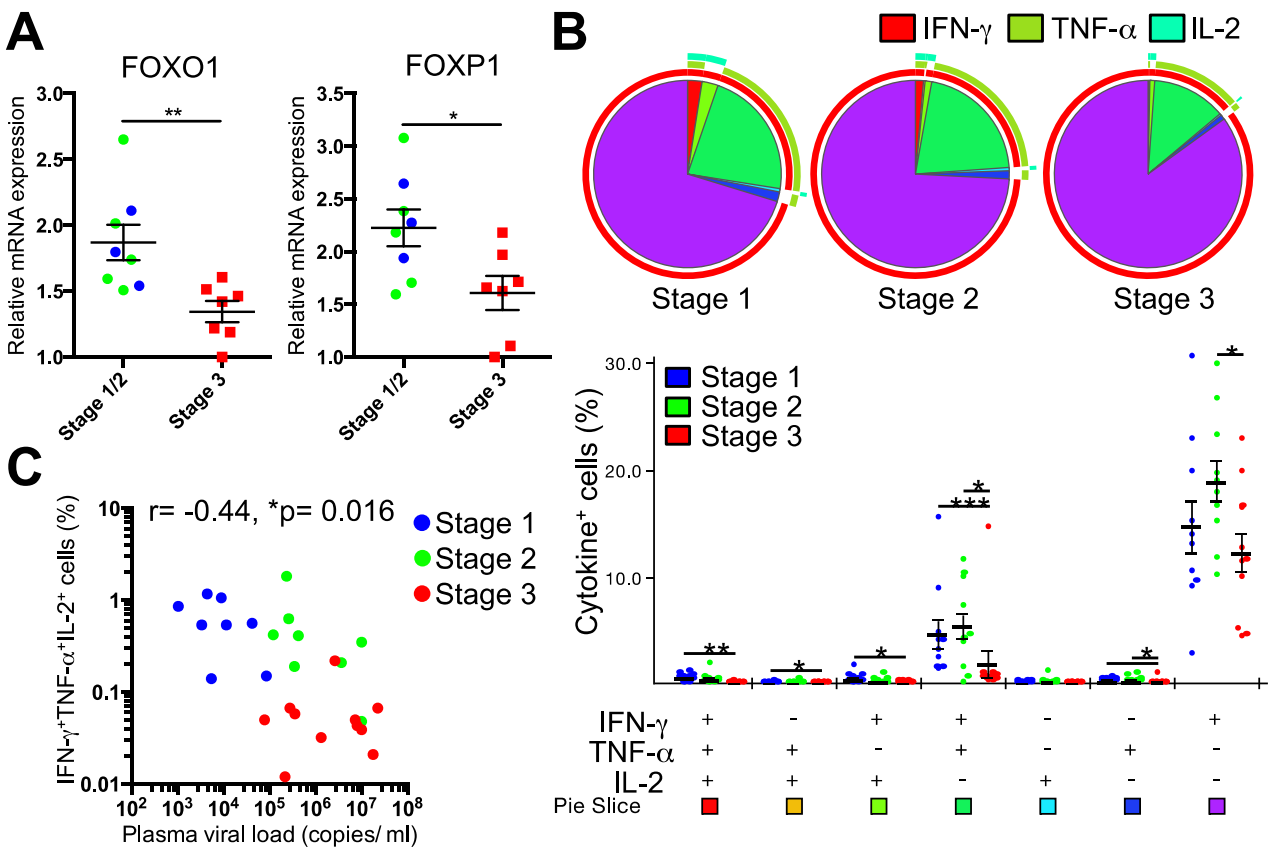

Fig. S4. Loss of memory potential and polyfunctionality of HIV-specific CD8$^+$ T cell in AHI. (A) mRNA expression of FOXO1 and FOXP1 in CD38$^+$HLA-DR$^+$ CD8$^+$ T cells from AHI stage 1/2 and 3 individuals. (B) Polyfunctionality of CD38$^+$HLA-DR$^+$ CD8$^+$ T cells stimulated with anti-CD3 and CD28 Ab analyzed for combination of cytokine productivity. (C) Correlation between plasma viral load and percentages of IFN-γ$^+$TNF-α$^+$IL-2$^+$ cells in CD38$^+$HLA-DR$^+$ CD8$^+$ T cells. Differences between groups were analyzed by Mann-Whitney tests. Associations between two variables (p and r) were analyzed by Spearman correlations. *P< 0.05; **P< 0.01; ***P< 0.001.

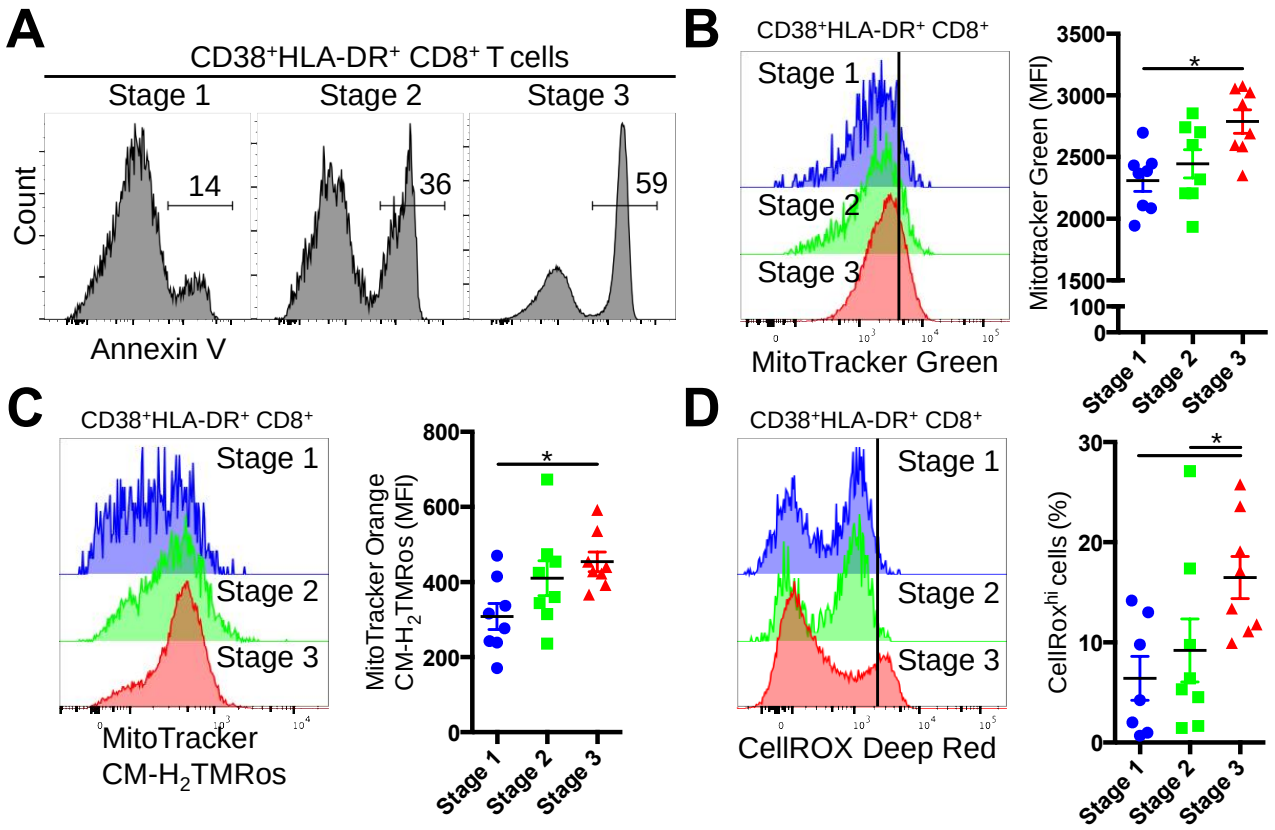

Fig. S5. Mitochondrial function of HIV-specific CD8$^+$ T cell during different stages of AHI. (A) Representative histograms of apoptotic Annexin V^{hi} cells in *ex vivo* CD38$^+$HLA-DR$^+$ CD8$^+$ T cells. (B) Mitochondria mass analysis based on MitoTracker Green accumulation in non-apoptotic CD38$^+$HLA-DR$^+$ CD8$^+$ T cells. (C) Mitochondria membrane potential analysis with MitoTracker Orange CM-H_2TMRos in non-apoptotic CD38$^+$HLA-DR$^+$ CD8$^+$ T cells. (D) Total reactive oxygen species level in non-apoptotic CD38$^+$HLA-DR$^+$ CD8$^+$ T cells based on incorporated CellROX Deep red oxidation. Differences between groups were analyzed by Mann-Whitney tests. *P< 0.05.

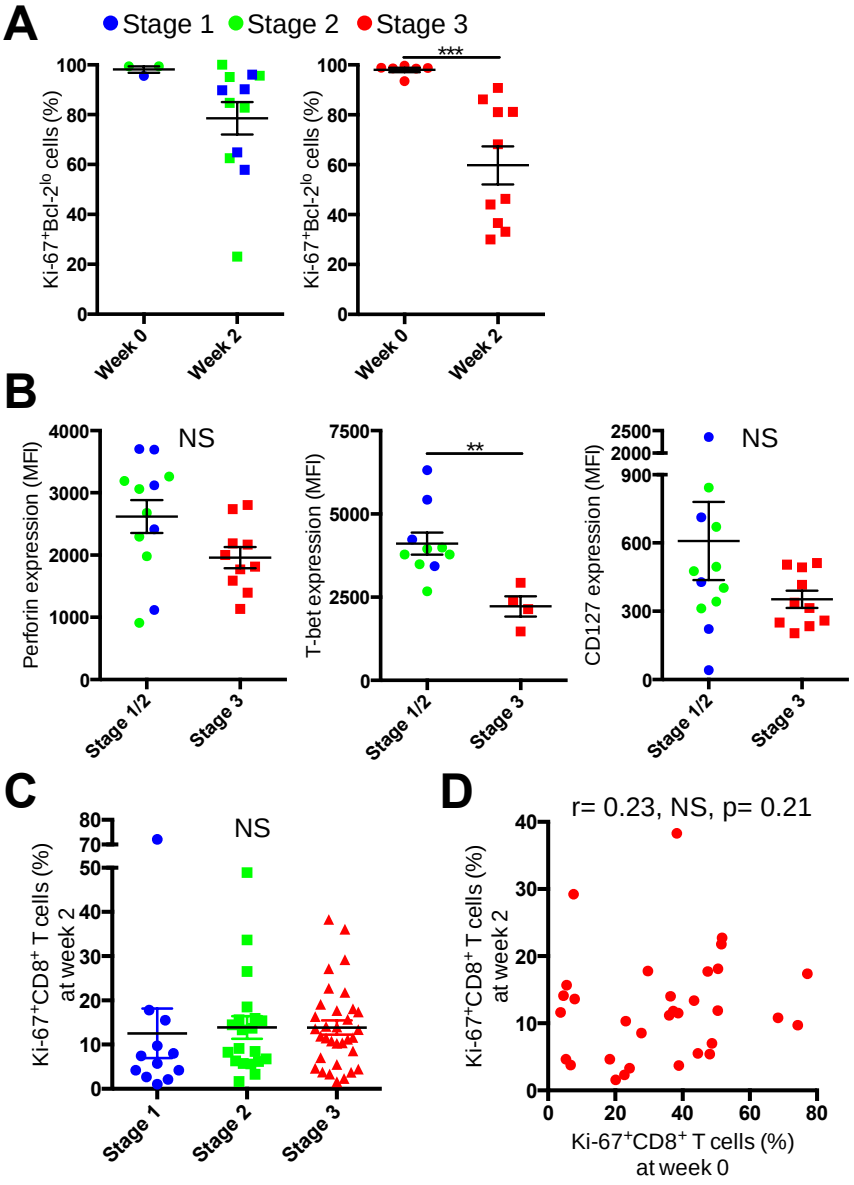

Fig. S6. HIV-specific CD8$^+$ T cells 2 weeks after ART initiation during AHI. (A) Percentage of Ki-67$^+$Bcl-2^{lo} cells in HIV-specific tetramer$^+$ CD8$^+$ T cells at week 0 and week 2 on ARV. (B) Expression of perforin, T-bet, and CD127 in/on HIV-specific tetramer$^+$ cells at week 2. (C) Percentage of Ki-67$^+$ cells in total CD8$^+$ T cells at week 2 after ART initiation. (D) Correlation between percentages of Ki-67$^+$ cells in total CD8$^+$ T cells from stage 3 individuals at week 0 and week 2. Differences between groups were analyzed by Mann-Whitney tests. Associations between two variables (p and r) were analyzed by Spearman correlations. **P< 0.01; ***P< 0.001.

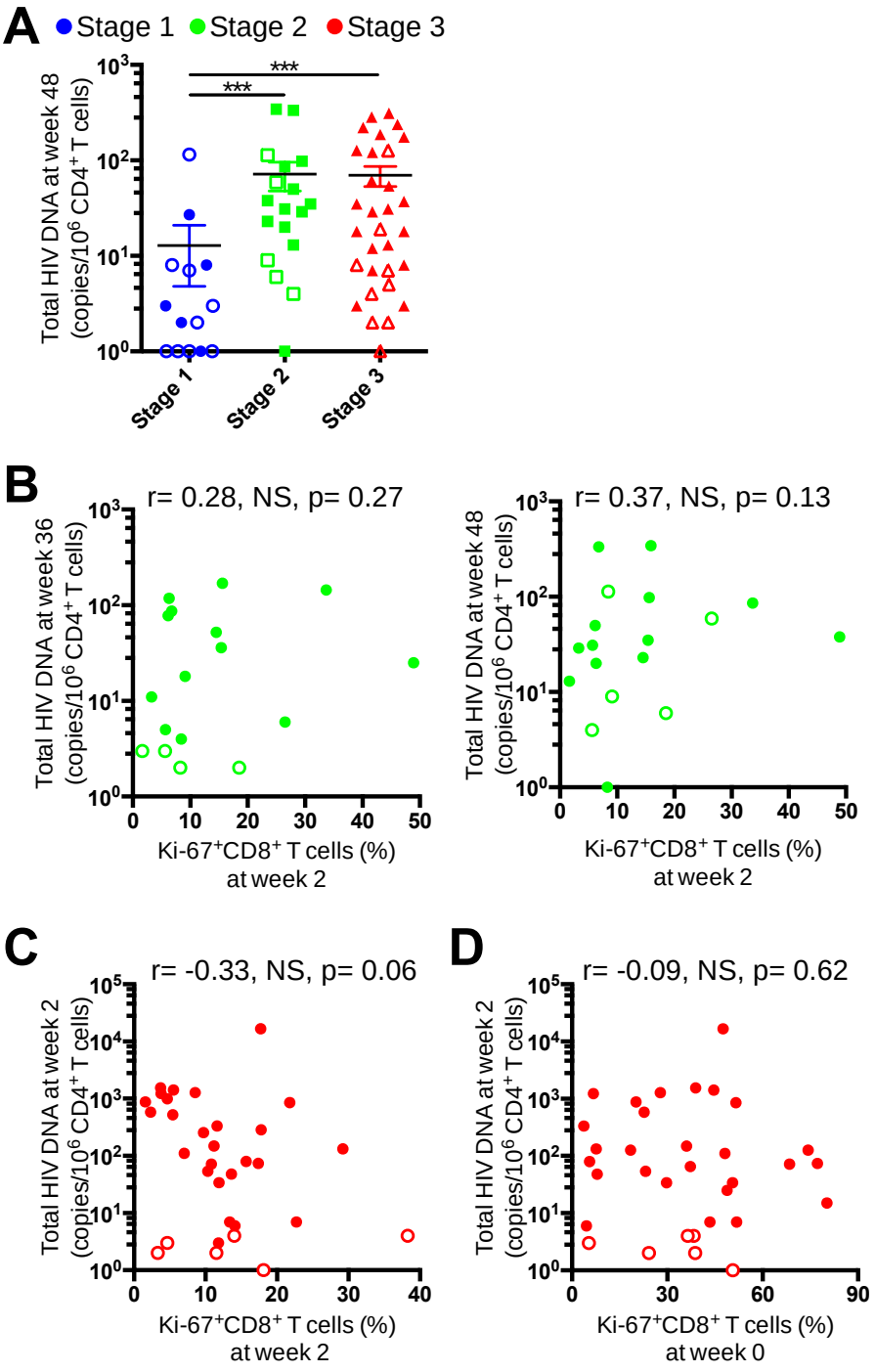

Fig. S7. Association between HIV-specific CD8$^+$ T cells and HIV reservoir after ART initiation during AHI. (A) Total HIV DNA copies/ 10^6 CD4$^+$ T cells among AHI stage 1-3 individuals at week 48. For samples in which no positive cells were detected, the limit of detection based on cell input is plotted as an open symbol. (B) Correlation between percentage of Ki-67$^+$CD8$^+$ T cells at week 2 and Total HIV DNA copies/ 10^6 CD4$^+$ T cells at week 36 and week 48 from AHI stage 2 individuals. (C) Correlation between percentage of Ki-67$^+$ cells in total CD8$^+$ T cells at week 2 and total HIV DNA copies/ 10^6 CD4$^+$ T cells at week 2 from AHI stage 3 individuals. (D) Correlation between percentage of Ki-67$^+$ cells in total CD8$^+$ T cells at week 0 and total HIV DNA copies/ 10^6 CD4$^+$ T cells at week 2 from AHI stage 3 individuals. Differences between groups were analyzed by Mann-Whitney tests. Associations between two variables (p and r) were analyzed by Spearman correlations. ***P< 0.001.

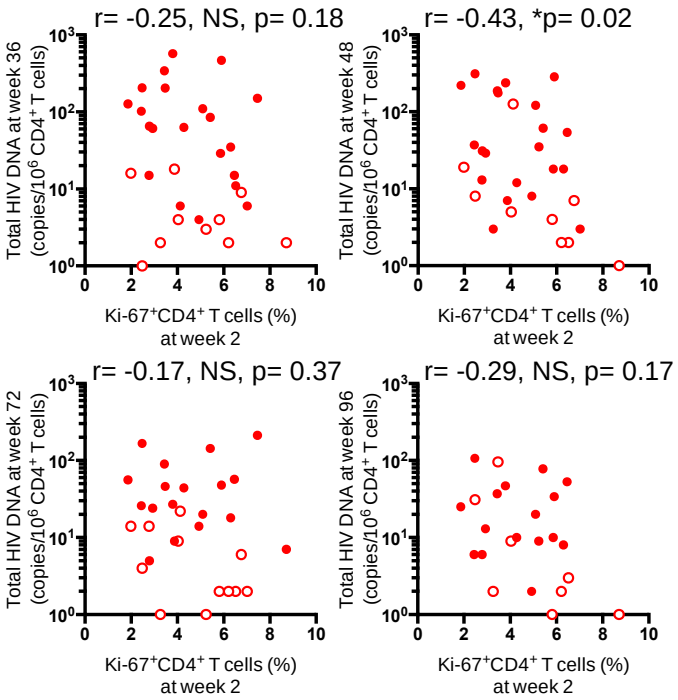

Fig. S8. Association between activated CD4$^+$ T cells and HIV reservoir after ART initiation during AHI. Correlation between percentage of Ki-67$^+$CD4$^+$ T cells at week 2 and Total HIV DNA copies/ 10^6 CD4$^+$ T cells at week 36, week 48, week 72, and week 96 in AHI stage 3 individuals. Associations between two variables (p and r) were analyzed by Spearman correlations. *P< 0.05.